Journal of Chromatography, 384 (1987) 25–44
Elsevier Science Publishers B.V., Amsterdam — Printed in The Netherlands

CHROMSYMP. 969

SIMPLIFIED DESCRIPTION OF HIGH-PERFORMANCE LIQUID CHROMATOGRAPHIC SEPARATION UNDER OVERLOAD CONDITIONS, BASED ON THE CRAIG DISTRIBUTION MODEL

I. COMPUTER SIMULATIONS FOR A SINGLE ELUTION BAND ASSUMING A LANGMUIR ISOTHERM

J. E. EBLE and R. L. GROB
Chemistry Department, Villanova University, Villanova, PA 19085 (U.S.A.)
P. E. ANTLE
Biomedical Products Department, E. I. Du Pont de Nemours & Co., Concord Plaza, Wilmington, DE 19898 (U.S.A.)
and
L. R. SNYDER*
LC Resources, Inc., 26 Silverwood Court, Orinda, CA 94563 (U.S.A.)

SUMMARY

High-performance liquid chromatographic separation in an overload mode has been studied using the Craig-distribution scheme, assuming a Langmuir isotherm. Elution curves were determined as a function of sample mass by computer simulation, for different values of both capacity factor (k') and column plate number (N) at low loading (k_0 and N_0). It was possible to generalize these data so as to correlate Craig elution curves with sample mass and other experimental conditions, through the definition of certain "loading functions": w_{xk} and w_{xN}. This led to a more rapid ("second generation") computer program for the prediction of elution curves for single compounds, as a function of sample mass, retention, and any plate number. Predictions by the latter approach agree well with the more time-consuming Craig simulations. This work provides a starting basis for studying overload high-performance liquid chromatographic separation as a function of sample size and experimental conditions. Later papers will show that (a) experimental data under overload conditions correlate well with the present model, and (b) the model can be extended to the case of two co-eluting solutes.

INTRODUCTION

Preparative separations by high-performance liquid chromatography (HPLC) are of increasing interest. Today this technique is often used to purify multi-gram quantities of various compounds, and some groups are carrying out separations at the kilogram and higher scale[1,2]. For such applications, the column will usually be

0021-9673/87/$03.50

operated in a "mass-overload" mode, such that sample retention and band-width are changed from what is observed under "analytical" (*i.e.*, small-sample) conditions[3]. Separation in an overload mode is usually much more complex than for the case of small-sample HPLC. A good deal of attention has been given to overload separations[4–20], but a comprehensive and convenient description of such procedures is not yet available. There is even considerable debate among experts as to whether analytical-scale separations can provide useful information for the design of corresponding overload separations.

There is a pressing need for a practical theory of overload HPLC that can be used for most separations, with a minimum of additional measurements, *e.g.*, no determination of sorption isotherms. The present two papers[21] plus reports to follow describe a new approach for understanding preparative HPLC under mass-overload conditions. We begin by using a model of chromatographic separation based on Craig-distribution[22] plus the assumption of Langmuir-isotherm retention[23]. This allows us to carry out computer-simulated HPLC separations under mass-overload conditions, for a single-solute sample. We then generalize the results of these computer simulations to arrive at simple relationships which give insight into overload-HPLC. These relationships also allow us to replace the time-consuming Craig simulations with second-generation computer simulations that require only a few minutes per run, regardless of column plate number. These results are described in the present paper.

In the following paper[21] we describe the extension of the above model to the case of non-Langmuir retention. We will show that a change in isotherm shape or type leads to an apparent reduction in the saturation capacity of the column, but often does not otherwise affect preparative separation. We will further show that an apparent column capacity (for a given HPLC system) is easily determined from a few overload experiments with small columns. This allows computer simulation of further runs under overload conditions. We will also show that experimental runs with a single solute (mass-overload conditions) are in reasonable agreement with our model. With minor, empirical adjustments in the starting Craig model, computer simulation can now be used to predict the effects of overload on the HPLC separation of a single band. Later papers will extend this treatment to the case of two co-eluting solutes.

COMPUTER SIMULATIONS

The Craig simulations were written in BASIC and executed on an IBM-XT (IBM, Boca Raton, FL, U.S.A.) with the use of a Microsoft BASIC compiler (Microsoft, Bellevue, WA, U.S.A.). Using the equations for a Langmuir isotherm (see Appendix I) and assigning the phase ratio $\psi = 0.1$, the fraction of solute in the mobile phase (r) was calculated as a function of total solute mass in both phases (for $k_0 = 1$, 3, and 10). Values of r *vs.* solute mass for each value of k_0 were then fit to an 8-term polynomial, using the General Statistics Pac (Hewlett-Packard, Palo Alto, CA, U.S.A.) on an HP-85 computer (Hewlett-Packard).

In our simulation algorithm, the sample is initially transferred to the mobile phase of the first cell. After equilibrating the two phases in the first cell, the fraction of solute in the mobile phase is calculated from the appropriate polynomial for r. The mobile phase is passed to the second cell, and fresh mobile phase is added to the

first cell. The two cells are again equilibrated, and the fraction of solute in the mobile phase of each cell is calculated as before. This process is repeated until 99.999% of the solute has left the last cell. Likewise, when the solute concentration in any cell decreases to 0.001% of the total injected sample-mass, that cell is ignored in further calculations. When the last cell is filled with mobile phase (after n transfers when the total number of cells, $n_c = n$), the solute mass in the mobile phase for this cell is transferred to an open file, as are subsequent transfers from the last cell. These data are equivalent to the calculated elution band. Calculations of k' and N were accomplished on the basis of both "band" and "cumulative" measurements (see Fig. 1 and below).

THEORY AND RESULTS

HPLC separations under analytical conditions generally approximate Gaussian elution bands with values of k' and N that do not vary with sample mass w_x (when w_x does not exceed a certain maximum value). Thus the shape and position of the band within the chromatogram remain fixed. When w_x is increased beyond some limit, values of the capacity factor k' and plate number N generally decrease with further increase in w_x, and the band becomes non-Gaussian (as measured by the peak asymmetry factor A_s)*. This is illustrated by reversed-phase HPLC runs for benzyl alcohol under analytical *vs.* overload conditions (0.94 mg injection, 5 × 0.46 cm column of Zorbax** C_8):

	Small sample	*0.94 mg*
k'	2.86	2.40
N	1836	241
A_s	1.0	3.3

Fig. 1a shows the benzyl alcohol band for this 0.94-mg sample.

Values of k' and N (in combination with derived overload parameters) determine the final separation under overload conditions. This is illustrated for Craig-simulated data in Fig. 8 of the present paper, and for experimental data in Figs. 26 and 27 of the following paper[21]. The following discussion is based on values of k' and N, and how these parameters vary with experimental conditions in overload separations. Overload values of k' and N can be measured in various ways. In Fig. 1a, k' is calculated from the retention time t_R (peak maximum, 95.7 s) and column dead time t_0 (28.2 s) in the usual way: $k' = 2.40$. Likewise, N is calculated from the bandwidth W_2 at 0.61 × band height (2σ, see p. 834 of ref. 3) and the retention time of 95.7 s: $N = (t_R/\sigma)^2$, or a value of $N = 241$ for the band of Fig. 1a.

Values of k' and N can also be determined from the derived cumulative elution (integral) plot of Fig. 1b. Here retention time is defined as the time when 50% of the solute has eluted from the column. Bandwidth is measured as the time difference between 15.9% and 84.1% elution, corresponding to $\pm 1\sigma$. Values of k' and N calculated in these two ways are slightly different for this overload separation (Fig. 1b *vs.* 1a). These differences become greater for increased sample size.

* For definitions of symbols used in these two papers, see the Glossary of symbols at the end of this paper. We define A_s in terms of the usual bandwidth measurements at 10% of peak maximum.

** Zorbax is a trademark of the Du Pont Company.

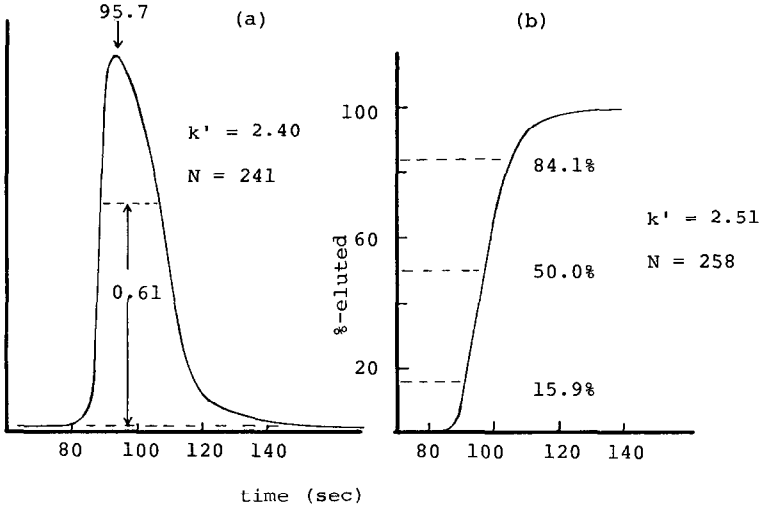

Fig. 1. Elution curves for a typical overloaded separation. Sample, benzyl alcohol, 0.94 mg injected; column 5 × 0.46 cm of C_{18} silica; mobile phase, methanol–water (40:60); flow-rate, 0.9 ml/min; temperature, 35°C (see ref. 21 for details). (a) elution curve from chromatogram; (b) cumulative elution calculated from (a) as described in ref. 21.

Sometimes we will find that the procedure of Fig. 1a is preferable for measurement of k' or N. More often we will use values of k' and N based on the cumulative elution curve (Fig. 1b). Fig. 2 shows two superimposed bands, separated under overload conditions, with an arbitrary cutpoint indicated by an arrow. In

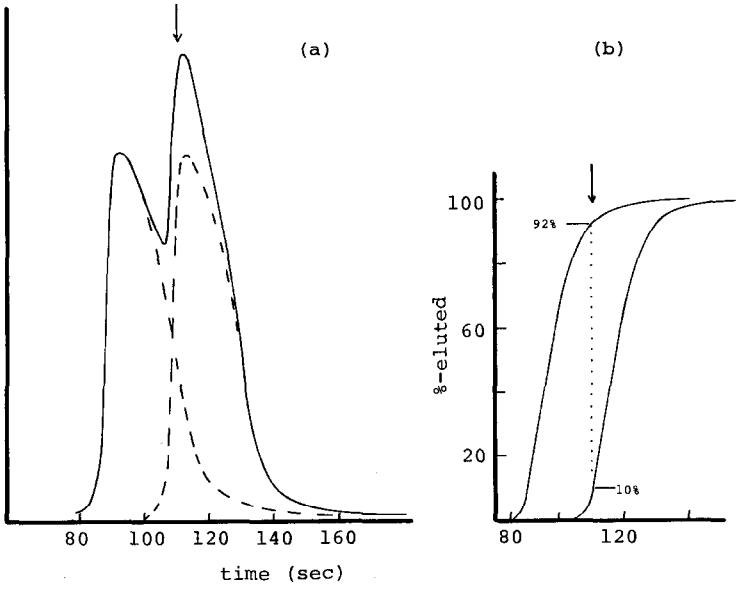

Fig. 2. Hypothetical elution curves for two overlapping bands under overload conditions. (a) From the chromatogram; (b) cumulative elution plots.

preparative HPLC, we are primarily interested in the yield and purity of fractions collected as illustrated in Fig. 2 (arrows). This information is more readily derivable from cumulative elution curves, as in Fig. 2b (92% yield of A in fraction 1, with a purity of 90%; assumes equal values of w_x for each band). We will refer to values of k' and N determined as in Fig. 1a as "band" values. Values of k' and N determined as in Fig. 1b will be referred to as "cumulative" values.

The Craig model

Attempts at creating a fundamental theory for overload HPLC have been reported by several workers. One of the more successful of these approaches is a perturbation model based on the mass balance equations that describe the concentrations of sample and mobile phase during separation (refs. 4, 5, 14, 16, 17 and related discussion in ref. 24). A Langmuir isotherm is assumed, and the model is limited to the case of moderate overloading of the column. Other approaches to predicting overload separation have also been described[10,11,15], but these appear less well developed, as well as more empirical. The major limitation of these treatments at the present time is that they apply only to the case of a single solute band. They are therefore unable to predict what will happen in the case of "real" separations, where two or more bands co-elute. We have therefore examined an alternative approach that will be shown applicable to the case of samples containing two or more components*.

The Craig distribution model, based on counter-current migration of a sample band in a train of equilibrated stages or "plates"[22], has often been used for illustrating or modeling chromatographic separation under non-overload conditions. The sample is placed in the first stage, and after equilibration of mobile and stationary phases, the mobile phase is then moved to the second stage; fresh mobile phase is added to the first stage, and the process is repeated. The process adequately describes the retention or equilibrium properties of the separation; the kinetic or band broadening characteristics can be represented by varying the number of stages in the system. The plate number N_0 (small sample) is related to the number of Craig stages n_c and capacity factor k_0 (small sample) as

$$N_0 = (n_c + 1)\,(k_0 + 1)/k_0 \qquad (1)$$

Early attempts at modeling overload separation in liquid–solid chromatography[25] via the Craig model showed promising results, but the speed of pre-1960 computers made simulations for large values of N impractical. More recently, the Craig model has been used to simulate band shapes for HPLC systems that exhibit tailing[26]. Using an IBM XT computer, we have been able to extend this approach to separations under overload conditions, for reasonably large values of both N (2000) and k'(10). These data suggest a simplified model of overload separation that allows the fast prediction of elution curves for any values of N and k'.

* In later papers we will show that the present model for mass overloaded separation of single-component samples can be adapted to the case of samples containing more than one component. The latter approach makes use of the concept of "column blockage", where one solute is regarded as effectively saturating some fraction of the stationary phase, thereby reducing the stationary phase or column length available for sorption of the second solute.

The Craig model is deficient in that no band broadening is predicted for the case of $k_0 = 0$. While this result is physically unrealistic, bands eluted at $k' = 0$ are of minimal interest. For $k_0 > 0$ the value of n_c can be adjusted to match the desired value of N_0; in the second paper[21] we will see that Craig-derived values of N (large samples) correlate well with experimental data as a function of sample size. In the following discussion, values of N or N_0 correspond to plate number measurements as in Fig. 1; values of n_c from the Craig simulations are also noted, but are not considered to be significant, except as they define values of N_0 (eqn. 1).

Langmuir isotherm simulations

Plate number N vs. sample mass. Initial simulations with the Craig model were carried out using classical Langmuir isotherms, which can be represented (Appendix I) as

$$1/w_{xs} = a + b/C_x \tag{2}$$

Here w_{xs} is the mass of solute in the stationary phase (g, for total column), and C_x is the concentration in the mobile phase (g/ml) at equilibrium. The constants a and b in eqn. 2 are given as

$$a = 1/w_s \tag{3}$$

and

$$b = 1/(V_m k_0) \tag{4}$$

The quantities k_0 and V_m refer, respectively, to the value of the capacity factor k' for small samples, and the column dead volume (equal to $[t_0 F]$; where F is the flow-rate). The saturation capacity w_s corresponds to the maximum solute uptake by the column when C_x is very large; it has also been referred to[27] as the "maximum loading capacity". A further discussion of the Langmuir isotherm is given in the following paper[21].

Computer simulations based on the Craig model ("Craig simulations") were next carried out for a broad range of conditions. Values of the Craig stage-number n_c were varied from 50 to 1000, the capacity factor (small samples) k_0 was varied from 1 to 10, and sample size was varied from the linear-isotherm region to heavily-overloaded separations. Values of k' and N were determined for each run, and the ratios k'/k_0 and N/N_0 were used to assess the effect of column overload on the separation. These results are reported in Table I and summarized in the plots of Figs. 3 and 4 (n_c values of 50–1000; $k_0 = 1$, 3, and 10) as a function of w_x/w_s, the fractional loading of the column by sample. The quantity w_x is the mass of sample injected into the column; $w_s = 0.1$ g in these examples. Values of N_0 ranged from 53 to 1965. It is seen (Figs. 3 and 4) that the relative overloading of the column, as measured by values of k'/k_0 or N/N_0, can occur at quite different sample sizes (w_x/w_s), depending on k_0 and N_0.

We next considered whether the data of Figs. 3 and 4 could be reduced to some simple relationships. The treatment of Poppe and Kraak[14] suggests for (a)

TABLE I

DATA FROM CRAIG SIMULATIONS OF OVERLOAD SEPARATION

Langmuir isotherms from eqns. 2–4 with ψ = 100 mg/ml, w_s = 100 mg, and V_m = 1.

n_c	N_0	k_0	w_x/w_s	w_{xk}	w_{xN}	k'/k_0		N/N_0	
						*cum**	*band**	*cum**	*band**
50	100	1	0.0001	0.0005	0.0025	1.00	1.00	1.00	1.00
			0.01	0.05	0.25	0.96	0.96	0.99	0.98
			0.03	0.15	0.75	0.90	0.88	0.95	0.93
			0.10	0.50	2.5	0.72	0.66	0.75	0.70
			0.30	1.5	7.5	0.46	0.32	0.43	0.36
			0.60	3.0	15	0.26	0.14	0.31	0.26
	65	3	0.001	0.006	0.036	1.00	1.00	1.00	1.00
			0.01	0.06	0.36	0.96	0.95	0.97	0.96
			0.03	0.18	0.11	0.88	0.85	0.87	0.82
			0.10	0.65	3.5	0.67	0.59	0.49	0.41
			0.20	1.2	7.3	0.51	0.38	0.27	0.20
			0.40	2.4	15.6	0.33	0.18	0.15	0.09
	53	10	0.0001	0.00066	0.0040	1.00	1.00	1.00	1.00
			0.003	0.02	0.13	0.99	0.99	0.99	0.99
			0.03	0.20	1.3	0.90	0.87	0.83	0.78
			0.06	0.4	2.6	0.78	0.71	0.55	0.47
			0.10	0.66	4.4	0.67	0.56	0.33	0.24
			0.20	1.3	8.8	0.49	0.33	0.14	0.07
			0.35	2.3	15	0.33	0.17	0.07	0.03
200	398	1	0.0005	0.005	0.050	1.00	1.00	1.00	1.00
			0.005	0.05	0.50	0.97	0.96	0.98	1.97
			0.02	0.20	2.0	0.88	0.84	0.80	0.77
			0.05	0.50	5.0	0.76	0.69	0.50	0.46
			0.10	1.5	15	0.56	0.43	0.22	0.19
	264	3	0.0002	0.0025	0.030	1.00	1.00	1.00	1.00
			0.005	0.061	0.74	0.96	0.95	0.94	0.93
			0.02	0.245	3.0	0.85	0.81	0.62	0.58
			0.05	0.61	7.4	0.73	0.65	0.30	0.25
			0.10	1.2	15	0.61	0.49	0.15	0.12
	216	10	0.0001	0.0013	0.018	1.00	1.00	1.00	1.00
			0.004	0.053	0.72	0.98	0.98	0.98	0.97
			0.01	0.13	1.8	0.94	0.94	0.86	0.83
			0.02	0.27	3.6	0.88	0.84	0.59	0.54
			0.03	0.40	5.4	0.83	0.77	0.40	0.35
			0.05	0.67	8.9	0.76	0.66	0.23	0.18
			0.08	1.1	14	0.67	0.54	0.13	0.09
			0.095	1.3	17	0.64	0.50	0.10	0.07
600	1193	1	0.0001	0.0017	0.030	1.00	1.00	1.00	1.00
			0.003	0.052	0.89	0.96	0.95	0.94	0.93
			0.01	0.17	3.0	0.90	0.87	0.67	0.65
			0.02	0.35	6.0	0.83	0.78	0.43	0.40
			0.03	0.52	8.9	0.79	0.72	0.31	0.29
			0.051	0.88	15	0.72	0.62	0.20	0.18

(*Continued on p. 32*)

TABLE I (*continued*)

n_c	N_0	k_0	w_x/w_s	w_{xk}	w_{xN}	k'/k_0		N/N_0	
						*cum**	*band**	*cum**	*band**
	790	3	0.0001	0.002	0.04	1.00	1.00	1.00	1.00
			0.001	0.021	0.44	0.99	0.98	0.98	0.97
			0.004	0.084	1.8	0.94	0.93	0.81	0.79
			0.01	0.21	4.5	0.89	0.85	0.49	0.46
			0.02	0.42	8.9	0.82	0.76	0.27	0.25
			0.034	0.72	15	0.76	0.68	0.16	0.14
	627	10	0.0001	0.0023	0.053	1.00	1.00	1.00	1.00
			0.01	0.23	5.3	0.91	0.88	0.52	0.49
			0.03	0.69	16	0.81	0.73	0.16	0.13
1000	1965	1	10–5	0.00022	0.0049	1.00	1.00	1.00	1.00
			0.005	0.11	2.5	0.93	0.92	0.73	0.72
			0.01	0.22	4.9	0.88	0.86	0.48	0.47
			0.02	0.44	9.9	0.82	0.77	0.28	0.26
			0.03	0.67	15	0.78	0.71	0.20	0.18
	1300	3	10–5	0.00003	0.0008	1.00	1.00	1.00	1.00
			0.0025	0.067	1.8	0.95	0.94	0.81	0.79
			0.005	0.14	3.6	0.92	0.90	0.56	0.55
			0.015	0.41	11	0.84	0.78	0.23	0.21

* Cum values calculated from cumulative elution curve as in Fig. 1b; band values from elution curve as in Fig. 1a.

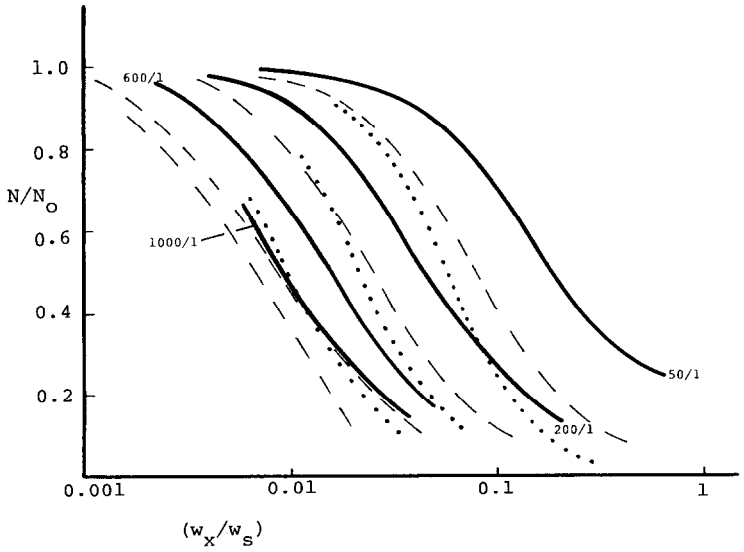

Fig. 3. Craig simulation data for plate number N as a function of sample size (w_x/w_s) and non-overload values of k' (k_0) and N (N_0). Numbers on curves, 100/1 indicates $N_0 = 100$ and $k_0 = 1$ (see Table I and text). Values of N_0 are "band" values, calculated as in Fig. 1a (not 1b). (– – –) $k_0 = 3$; (· · · ·) $k_0 = 10$.

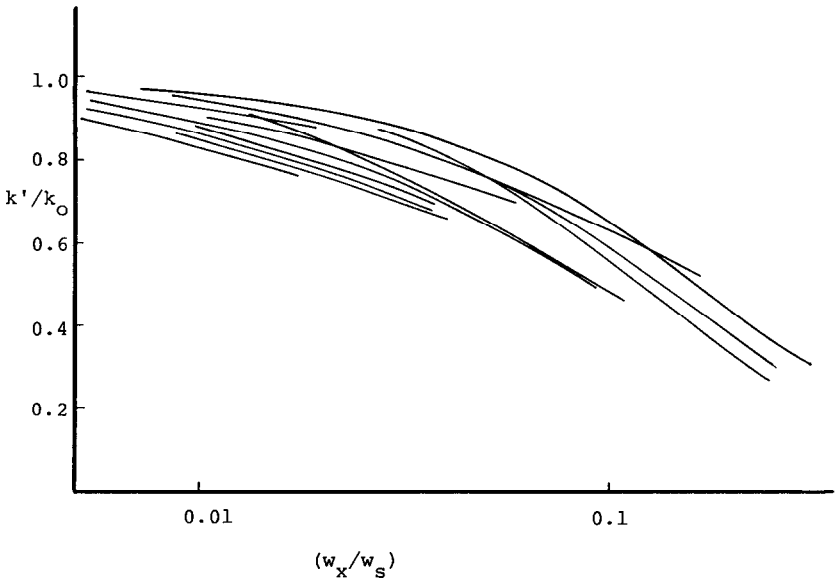

Fig. 4. Craig simulation data for capacity factor k' as a function of sample size (w_x/w_s) and non-overload values of k' (k_0) and N (N_0). See data of Table I. Values of k' are "band" values, calculated as in Fig. 1a (not 1b).

moderate overloading of the column, and (b) a Langmuir isotherm, that N/N_0 will be defined by some function of N_0, k_0, and w_x/w_s

$$\begin{aligned} N/N_0 &= \mathrm{f}\{N_0[k_0/(1+k_0)]^2\ w_x/w_s\} \\ &= \mathrm{f}\{w_{xN}\} \end{aligned} \tag{5}$$

Here we define $w_{xN} = N_0[k_0/(1+k_0)]^2\ w_x/w_s$: w_{xN} is the "loading function" for N/N_0 as a function of sample size. The data of Fig. 3 are replotted against w_{xN} in Fig. 5; as expected from ref. 14, the values of N/N_0 now cluster about a single curve. That is, use of the loading function w_{xN} allows us to predict values of N/N_0 for any combination of values of N_0, k_0 and w_x/w_s, using the master curve (solid line) of Fig. 5. This master curve is the best fit to data for large N_0 (see below). Note that w_{xN} can be regarded as the mass of sample X contained in the stationary phase of the first Craig stage.

While the treatment of Poppe and Kraak[14] and eqn. 5 have been derived for the case of moderate column overloading, we will show that this relationship (eqn. 5) is reasonably accurate for samples large enough to effect a 90% reduction in values of N.

Capacity factor k' vs. sample mass. The effect of sample overload on k' is related to the average sample concentration in the stationary phase during migration of the band through the column. That is, the instantaneous value of k' during migration of the band through the column will vary (approaching k_0 as the sample becomes more dilute), depending on the mass of sample in a given plate (*i.e.*, sample

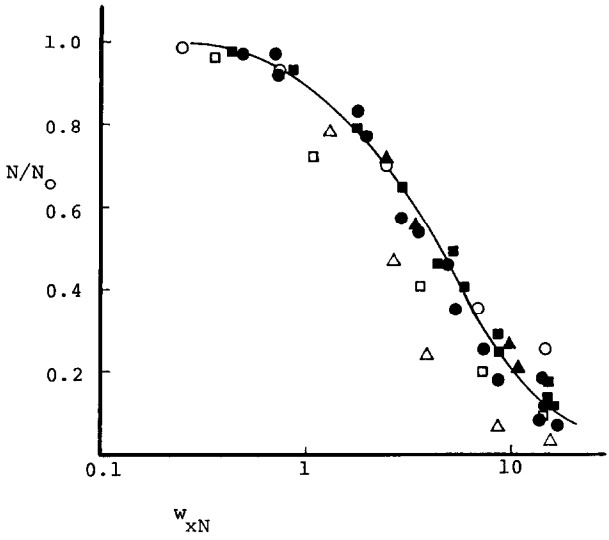

Fig. 5. Correlation of values of N/N_0 with column loading function w_{xN}.

n_c	k_0		
	1	*3*	*10*
50	○	□	△
200	●	●	●
600	■	■	■
1000	▲	▲	

Values of N are "band" values, calculated as in Fig. 1a (not 1b). The solid curve is drawn through data-points for $N_0 \geqslant 200$.

concentration at each point within the column). The resulting k' value at elution will then be (roughly) the average of k' values for the band maximum at every point along the column, which is in turn related to the average concentration of solute in the stationary phase (w_{xs}; *cf.* eqn. 4-1 of ref. 23). We can obtain an inferential relationship between the average k' value and experimental conditions (including sample size) as follows. The band-maximum concentration of sample in the stationary phase will be proportional to the fraction of total solute in the stationary phase, equal to $k'/(1+k')$. This solute concentration will also be inversely proportional to band width; *i.e.*, proportional to $N^{0.5}$. This suggests, by analogy with eqn. 5, that

$$\begin{aligned} k'/k_0 &= \mathrm{f}\{N_0^{0.5}\,[k_0/(1+k_0)]\,w_x/w_s\} \\ &= \mathrm{f}(w_{xk}) \end{aligned} \tag{6}$$

Here the loading function w_{xk} equals $[k_0/(1+k_0)]\,N_0^{0.5}$. Eqn. 6 suggests that column overload, as measured by values of k'/k_0, is determined by the value of the loading factor w_{xk}; *i.e.*, plots of k'/k_0 *vs.* w_{xk} should fall on a single curve for various values of k_0, N_0 or w_x/w_s. Fig. 6 replots the data of Fig. 4 as k'/k_0 *vs.* w_{xk}, and shows (as

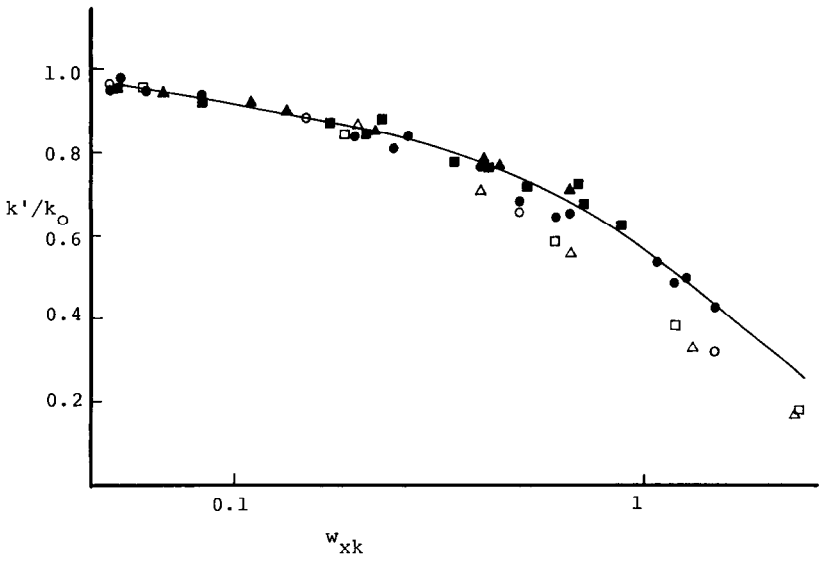

Fig. 6. Correlation of values of k'/k_0 with column loading function w_{xk}. Same symbols as in Fig. 5. Values of k' are "band" values, calculated as in Fig. 1a (not 1b). the solid curve is drawn through data points for $N_0 \geqslant 200$.

in Fig. 5) that all the data cluster about a single curve that can be used to predict k'/k_0 as a function of experimental conditions.

It appears that eqns. 5 and 6 become progressively more reliable for larger values of N_0, as summarized below:

Variable	*x-axis scatter in plotted values*		
	vs. w_x	*vs.* w_{xk}, w_{xN}	
		All data	$N_0 \geqslant 200$
N	40×	4×	1.2×
k'	4×	2×	1.3×

That is, for $N_0 \geqslant 200$, the scatter in the data is equivalent to an uncertainty of only 20–30% in sample size (or values of the loading factor)*. Values of N_0 in preparative HPLC will usually exceed 200; we have therefore drawn the curves of Figs. 5 and 6 through data points for $N_0 \geqslant 200$. The reduced accuracy of eqns. 5 and 6 for small N_0 ($n_c < 200$) is probably the result of increasing differences in Craig distribution *vs.* continuous chromatography as a stage or plate occupies a larger fraction of the total column.

For the case of systems following the Langmuir isotherm (eqn. 2), Figs. 5 and

* That is, when the solid curves of Figs. 5 or 6 are shifted horizontally by *ca.* 20–30%, they overlap most of the data points for $N_0 \geqslant 200$. This reflects the error in values of k'/k_0 or N/N_0 that are predicted from the solid curve.

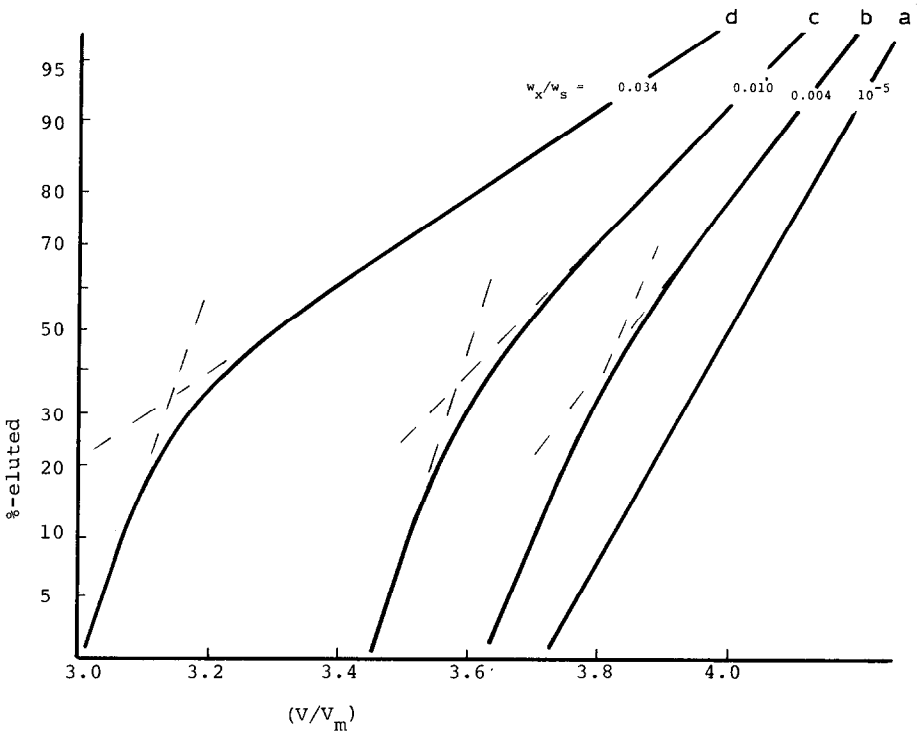

Fig. 7. Shape of cumulative elution band as a function of column overloading (see text). n_c = 600, k_0 = 3 (Table I).

6 suggest that we can predict k' and N in preparative HPLC as a function of k_0, N_0 and w_x/w_s. So far, we have only considered computer simulation (Craig model) data, but in the following paper we will see that this is true for experimental data as well. Thus, we can determine k_0 and N_0 from an initial analytical-scale run, and values of w_s can then be determined in various ways, as described in the following paper[21].

Band shape vs. sample size. We desire to predict the cumulative elution curve (as in Fig. 1b) as a function of sample size and other experimental conditions. This curve is related to values of k' and N, which can be predicted as above for overload separations. However, band shape also changes with overload, and we must take this into account. We have found that various measures of band shape (*e.g.*, band asymmetry) correlate well with the loading function w_{xN}, suggesting a simple approach for predicting band shape as a function of sample size (Appendix II).

Fig. 7 shows some representative examples of cumulative-elution curves* for varying sample size, taken from a series of Craig simulations where only sample size was varied. Curve a shows a non-overloaded run, with the data falling on a single straight line. This is expected for a Gaussian band, when plotted on "probability

* These plots of Fig. 7 are on "probability paper". The *y*-axis is labeled "cumulative %", but is linear in units of σ (standard deviation) of the Gaussian curve. Thus, 50% corresponds to $\sigma = 0$, 16% to $\sigma = -1$, 84% to $\sigma = +1$, etc. Any "true" Gaussian distribution will therefore plot as a straight line on probability paper.

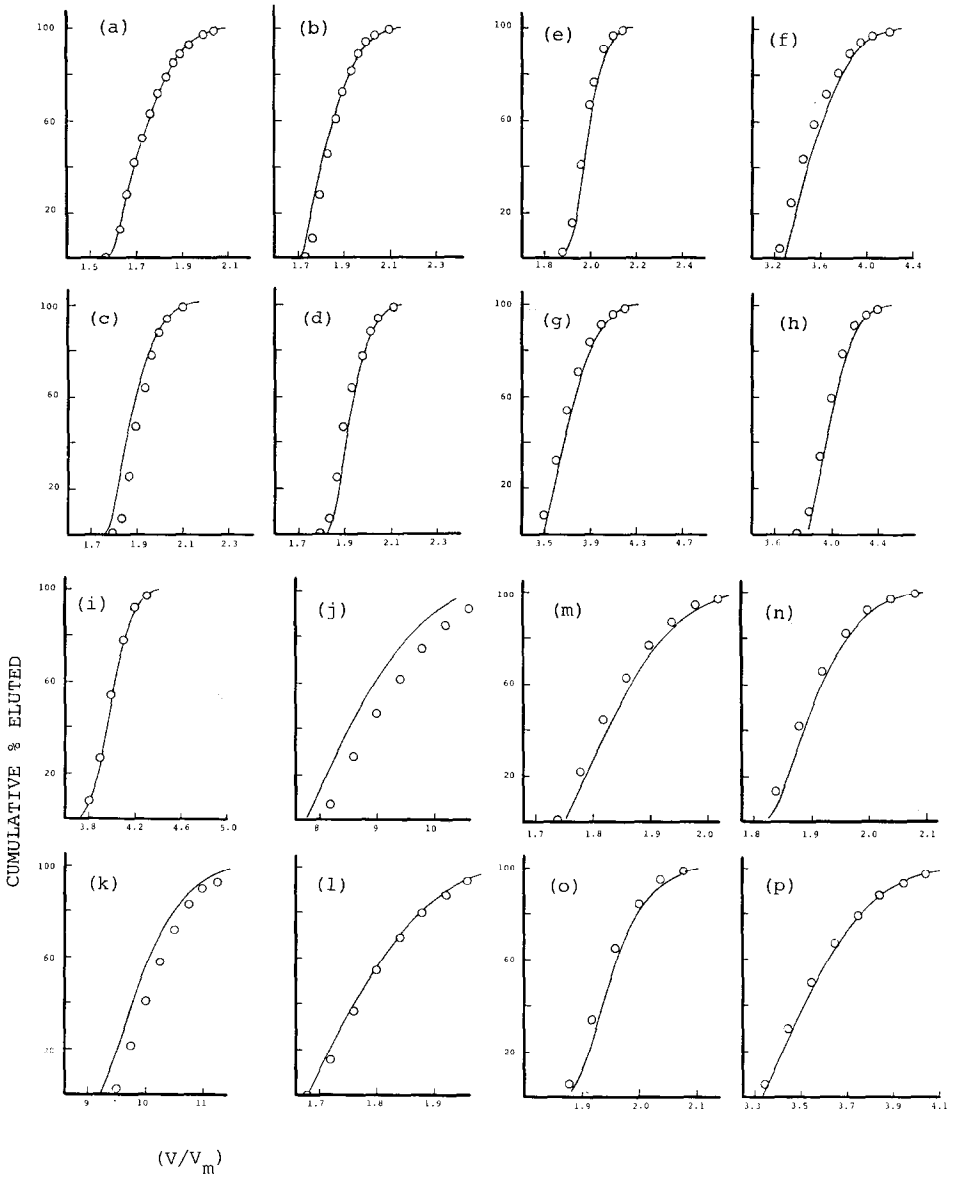

Fig. 8. Prediction of elution curves (Craig simulation, Langmuir isotherm, data of Table I) based on relationships of Table II (cumulative values) and procedure of Appendix I (see text). ○, Craig simulations; ——, model simulations.

Curve	n_c	k_0	w_x/w_s	*Curve*	n_c	k_0	w_x/w_s
a	600	1	0.051	j	600	10	0.030
b			0.030	k			0.010
c			0.020	l	1000	1	0.030
d			0.010	m			0.020
e			0.003	n			0.010
f		3	0.020	o			0.005
g			0.010	p		3	0.015
h			0.004				
i			0.001				

paper". Curves b–d show that, as overloading of the column increases, there is increasing deviation of the cumulative elution curve from a Gaussian distribution.

Cumulative elution curves as in Fig. 7 characteristically exhibit two distinct parts, where the initial part of the elution curve follows a steeper, roughly linear plot and the final part of the curve follows a shallower, roughly linear plot. That is, such elution curves appear to be a composite of parts from two separate Gaussian curves: one describing the first part of the elution band, and one describing the last part. The slopes and points of intersection of these two straight-line curves correlate well with the loading function w_{xN}, over a broad range of choices of k_0, N_0 and w_x/w_s. That is, the overall shape of the elution band appears to be defined by the value of w_{xN}.

It is possible to generalize these observations relating to Fig. 7, and to predict the shape of the elution band as a function of experimental conditions (k_0, N_0, w_x and w_s). These relationships are summarized in Appendix II. Combining these equations with the correlations of Figs. 5 and 6 then allows prediction by computer of the entire elution curve (Craig model, Langmuir isotherm) for any experimental conditions (any values of k_0, N_0, w_x and w_s), but without repeating an actual Craig simulation. We will refer to such simplified calculations as "model simulations". Several examples of model simulations are compared with Craig simulations in Fig. 8, with good agreement between the two simulations. The advantages of bypassing the actual Craig simulations include:

(1) Craig simulations for N_0 values > 1000 require a prohibitive amount of

TABLE II

BEST-FIT VALUES OF N/N_0 AND k'/k_0 *vs.* THE VARIOUS LOADING FUNCTIONS

Data from Figs. 5 and 6 and Table I

w_{xN} *or* w_{xk}	N/N_0	k'/k_0	
	*Cum**	*Band*	*Cum***
0.01	1.00	1.00	1.00
0.02	1.00	0.99	0.99
0.05	1.00	0.97	0.97
0.10	1.00	0.93	0.95
0.20	1.00	0.86	0.90
0.50	0.98	0.74	0.81
1.0	0.93	0.57	0.70
2.0	0.80	0.33	0.45
5.0	0.48		0.18
10	0.26		0.07
20	0.14		
50	0.06		
100	0.03		

* Data can be fit by the following polynomial in $x = \log w_{xN}$, within the limits of $0.5 < w_{xN} < 20$: $N/N_0 = 0.9308 - 0.2779\,x - 0.5098\,x^2 - 0.3252\,x^3 + 0.3127\,x^4 + 0.3275\,x^5 - 0.1434\,x^6 - 0.0946\,x^7 + 0.0394\,x^8$.

** Data can be fit by the following polynomial in $x = \log w_{xk}$, within the limits of $0.02 < w_{xk} < 5$: $0.6857 - 0.6427\,x - 0.6453\,x^2 + 0.1303\,x^3 + 0.8568\,x^4 + 0.3653\,x^5 - 0.3270\,x^6 - 0.2867\,x^7 - 0.0591\,x^8$.

time for small computers (*e.g.*, the IBM XT); model simulations (Appendix II) require less than 1 min per run for any value of N_0.

(2) The value of N_0 for each solute in a model simulation can be assigned, whereas these values are fixed in Craig simulations according to eqn. 1.

(3) The generalized correlations of Figs. 5, 6 and Appendix II allow better insight into the effects of different variables on preparative separation; we will show this in later papers.

Table II summarizes values of N/N_0 *vs.* w_{xN} and k'/k_0 *vs.* w_{xk} (solid curves of Figs. 5 and 6) for use in model simulations, as described in Appendix II.

DISCUSSION AND CONCLUSIONS

Considerable simplification has been achieved so far in describing how an elution band changes with column overload. For the case of Langmuir-isotherm Craig-simulation runs, we have shown that the resulting changes in the elution curve can be predicted from a knowledge of (a) the elution band under non-overload conditions (values of k_0 and N_0) and (b) sample size in relation to column saturation capacity (w_x/w_s). The comparisons in Fig. 8 show our ability to predict the final elution band (as obtained by Craig simulation), using the much faster "model simulations". The expanded scale of the x axis of Fig. 8 should be noted, as it exaggerates errors in predicted data points.

Previous workers[8,26] have noted that columns can be overloaded with respect to plate number N, while the capacity factor k' remains unchanged. This becomes more noticable with decrease in size of the column packing particles[8,12]. The present analysis confirms (as noted in ref. 12) that particle size *per se* is not the critical factor in these obervations; rather it is the actual value of N under non-overload conditions (N is usually larger for small-particle columns).

We can calculate the value of (w_x/w_s) equal to the fractional saturation of column capacity required to reduce both N and k' by some arbitrary amount (*e.g.*, 20%), as a function of N_0 (value of N for non-overload separation). These results are shown in Table III. Also shown are approximate weights for a typical preparative

TABLE III

SAMPLE SIZE REQUIRED TO REDUCE k' or N BY 20% (*VS.* VALUES OF k_0 AND N_0 — NON-OVERLOAD SEPARATION)

k_0 = 3. Data of Figs. 5 and 6.

N_0	w_x/w_s *for 20% reduction in* k'	w_x/w_s *for 20% reduction in* N	*mg sample**	
			k'	N
100	0.07	0.04	730	420
300	0.04	0.01	450	105
1000	0.02	0.004	210	42
10 000	0.007	0.0004	70	4
100 000	0.002	0.00004	21	0.4

* For 20% reduction in k' or N; assumes 10.5 g for w_s; *e.g.*, 25 × 2.1 cm column, 300 m²/g surface area.

column (25 × 2.1 cm, $w_s \approx 10.5$ g). For small-N columns ($N < 1000$) we see that both k' and N will decrease when the sample size exceeds some maximum value. However, for more efficient columns ($N \geqslant 10000$), larger samples will result in a decrease in N long before any change in k' is apparent (*cf.* also Figs. 3 and 4).

APPENDIX I

Derivation of Langmuir isotherm

The Langmuir isotherm assumes an adsorbed monolayer for the stationary phase, with one molecule of solute (X) replacing one adsorbed molecule of mobile phase (M) during retention of the solute. This leads to the general equation (*e.g.*, 23)

$$\theta_x = K N_x/(1 + K N_x) \tag{A1}$$

where θ_x is the mole fraction of solute in the adsorbed monolayer and N_x is the mole fraction of X in the mobile phase; K_x is the thermodynamic distribution coefficient for X. Eqn. A1 assumes that $N_x \ll 1$. If we further assume that the density and molecular weight of molecules of M and X are the same for each compound, then

$$\theta_x = w_{xs}/w_s \tag{A2}$$

and

$$N_x = w_{xm}/V_m = C_x \text{ (g/ml)} \tag{A3}$$

Here w_{xs} and w_{xm} are the weights of X in the stationary and mobile phases, respectively, w_s is the weight of an adsorbed monolayer of X, V_m is the volume of mobile phase within the column (column dead-volume), and C_x is the concentration of X in the mobile phase (g/ml).

Eqns. A1–A3 combine to give

$$1/w_{xs} = 1/w_s + (1/w_s)\,[1/(K C_x)] \tag{A4}$$

For small values of θ_x and N_x, we have (eqns. A1–A3)

$$K = (w_{xs}/w_s)\,(1/C_x) \tag{A5}$$

and

$$k_0 = w_{xs}/(V_m C_x) \tag{A6}$$

We can define the phase ratio

$$\psi = w_s/V_m \tag{A7}$$

and eqns. A5 and A6 then give

$$K = k_0/\psi \tag{A8}$$

Now eqns. A4 and A8 yield

$$1/w_{xs} = 1/w_s + [1/V_m k_0)] (1/C_x)$$

$$= a + b (1/C_x) \quad \text{(A9)}$$

The parameters a and b are fixed for a given HPLC system, with

$$a = 1/w_s \quad \text{(A10)}$$

and

$$b = 1/V_m k_0 \quad \text{(A11)}$$

The units for the various quantities above may appear confusing, until it is recalled that our derivation assumes that the densities of solute and mobile phase are the same. Therefore concentration C_x (g/ml) is equivalent to (g/g). See the Glossary of symbols for preferred units for each quantity.

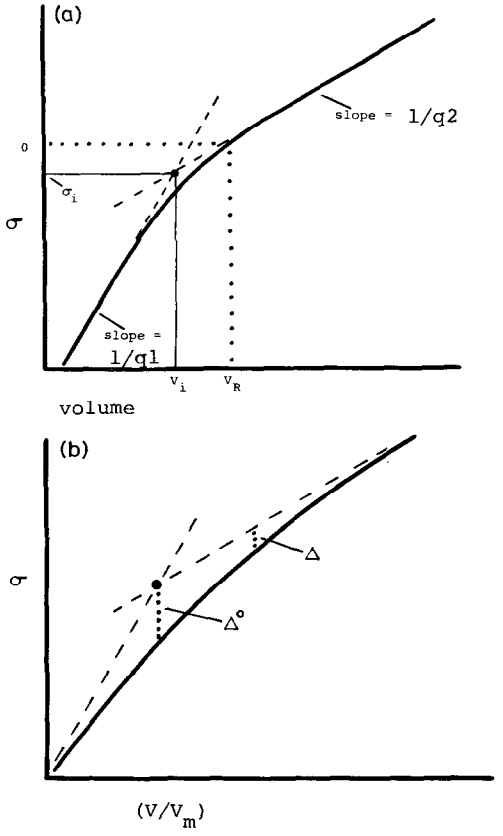

Fig. A1. Illustration of cumulative elution curve under overload conditions and empirical parameters used to predict the elution curve (*cf.* Fig. 7 and Appendix II). (a) Full elution curve; (b) magnified portion of (a).

APPENDIX II

Empirical description of overload elution curves

The characteristic cumulative elution curves of Fig. 7 can be represented generally by the diagram of Fig. A1. The two linear parts of the elution curve are shown, along with the volume corresponding to intersection of the two linear curves (V_i), the corresponding Gaussian standard deviation σ_i, and the retention volume V_R (either "band" or "cumulative"). The slopes of the two curves as measured from $\sigma = 0$ to $\sigma = -1$ and $+1$ are defined as $1/q_1$ and $1/q_2$, respectively. In each case, the slopes are equal to $d\sigma/dV_R$, where V_R is elution volume. We can regard the total elution curve as the sum of two separate elution curves; one with a larger N-value and smaller bandwidth (q_1, volume units/σ), and the other with a smaller N value and a larger bandwidth (q_2).

Fig. A1b shows an expanded view of Fig. A1a; here we further define the deviation of the actual (solid) elution curve from the dashed linear curves by the quantity Δ, and likewise the maximum value of Δ at V_i can be defined: Δ^0.

We have studied the dependence of each of the parameters of Fig. A1 (Δ, q_1, q_2, etc.) on separation conditions (runs of Table I), and found that these parameters can be empirically correlated with known properties of the system as follows:

$$\sigma_i = 0.14\, w_{xN}^{0.55} \tag{A12}$$

$$q_2/q_1 = 1 + 0.72\, w_{xN}^{0.70} \tag{A13}$$

$$\Delta^0 = 0.16\, w_{xN}/(1 + 0.4\, w_{xN}) \tag{A14}$$

$$\Delta = \Delta^0\, 10^{-1.2(\sigma - \sigma_i)} \tag{A15}$$

The average band width (σ_v, volume units) can be calculated from the plate number N (assumes a Gaussian):

$$\sigma_v = V_R\, N^{0.5} \tag{A16}$$

The inverse slopes of the linear plots in Fig. A1 are equal to q_1 and q_2, respectively. Since values of N are measured from bandwidth as defined for ± 1 standard deviation around the 50% elution point (cumulative values), we then have

$$2\,\sigma_v = (1-\sigma_i)q_1 + (1+\sigma_i)q_2 \tag{A17}$$

Values of q_1 and q_2 are then obtainable from eqns. A16 and A17 and previously determined values of N and (q_2/q_1).

Knowing the value of V_R at $\sigma = 0$ from the w_{xk} function and knowing the slope, $1/q_2$, the retention volumes at points greater than $\sigma = 0$ are calculated. The volume corresponding to σ_i is calculated from $V_i = V_R$ (at $\sigma = 0$) $+ \sigma_i\, q_2$. Volumes at smaller σ are calculated using the slope q_1. The two resulting straight lines are then curved by subtracting the corresponding value from each σ.

Once the elution curve is calculated, the value of V_R is checked against the original value determined from k':

$$V_R = V_m (1+k') \quad \text{(A18)}$$

Generally the calculational procedure will have introduced a small shift in the curve along the x-axis, so that the final value of V_R is slightly in error. The final step is then to shift the elution curve to correct for this effect and generate a final curve with a value of V_R that matches that calculated from the input value of k' (eqn. A18).

GLOSSARY OF SYMBOLS

For both this and the following papers; I- or II- is used for reference to specific equations; thus, I-6 refers to eqn. 6 of Part I)

a	constant in eqn. I-2; equal to $1/w_s$ (g^{-1})
a_1, a_2	value of a for sites of Type 1 or 2; eqns. II-3 and 4
A_s	band asymmetry factor[3]
b	constant in eqn. I-2 (ml^{-1}); equal to $1/(V_m k_0)$
b_1, b_2	value of b for sites of Type 1 or 2; eqns. II-3 and 4
"band"	refers to values of k' or N measured as in Fig. I-1a
Craig simulation	refers to predictions of k', N or band shape by carrying out computer simulations based on Craig distribution
C_x	solute concentration in the mobile phase (mg/ml)
"cumulative"	refers to values of k' or N measured as in Fig. I-1b
f( )	a function of ( )
k'	capacity factor[3]; "band" values of k' measured as in Fig. I-1a; "cumulative" values measured as in Fig. I-1b
k_0	value of k' for a small solute mass; constant as solute size is varied within a certain range
K	thermodynamic distribution constant for retention of solute; eqn. I-A1
L	column length (cm)
M	a molecule of mobile phase; eqn. II-1
model simulation	refers to prediction of k', N or band shape using the simplified model of Appendix II
n	stoichiometry factor for retention process; eqn. II-2
n_c	number of stages in a Craig simulation; eqn. I-1
N	column plate number[3]; "band" values of N, measured as in Fig. I-1a; "cumulative" values measured as in Fig. I-1b
N_x	mole fraction of solute in the mobile phase; eqn. I-A3
N_0	value of N for a small solute mass; constant within a certain range of sample size
SA	surface area (m^2/g) of column
V_m	column dead-volume (ml) (ref. 3)
V_s	column saturation capacity, measured as solute volume; eqn. II-6
V_R	retention volume (ml), measured as "cumulative" value
w_s	column saturation capacity (mg); maximum column loading at large values of C_x

w_{xk}	loading function for a given capacity factor as a function of sample size and conditions; equal to $N_0^{0.5}$ $[k_0/(1+k_0)]$ (w_x/w_s)
w_{xm}	mass of solute in the mobile phase (mg)
w_{xN}	loading function for a given plate number as a function of sample size and conditions; equal to $N_0[k_0/(1+k_0)]^2$ (w_x/w_s)
w_x	total mass of solute injected into the column (mg)
w_{xs}	mass of solute in the stationary phase (mg); eqn. I-2
w_1, w_2	value of w_{xs} for sites of Type 1 of 2; eqn. II-3
X	a molecule of solute; eqn. II-1
θ_x	mole fraction of solute in the stationary phase; eqn. I-A1
Δ,Δ^0	quantities defined in Fig. I-9b
σ	one standard deviation of a Gaussian-shaped band
σ_i	defined from the intersection of two lines as in Fig. I-9a
σ_v	one standard deviation of a Gaussian-shaped band; measured in ml in Appendix I-II
q_1, q_2	reciprocal slopes of initial and final plot, as in Fig. I-9a; values of σ for the two parts of the band
ψ	phase ratio (mg/ml); eqn. I-A7

REFERENCES

1 A. M. Cantwell, R. Calderone and M. Sienko, *J. Chromatogr.*, 316 (1984) 133.
2 H. Colin, G. Lowy and J. Cazes, *Am. Lab.*, 17 (1985) 139.
3 L. R. Snyder and J. J. Kirkland, *Introduction to Modern Liquid Chromatography*, Wiley-Interscience, New York, 2nd ed., 1979, Ch. 15.
4 G. Houghton, *J. Phys. Chem.*, 67 (1963) 84.
5 P. C. Haarhoff and H. J. van der Linde, *Anal. Chem.*, 38 (1966) 573.
6 J. J. De Stefano and H. C. Beachell, *J. Chromatogr. Sci.*, 10 (1972) 654.
7 K. J. Bombaugh and P. W. Almquist, *Chromatographia*, 8 (1975) 109.
8 J. N. Done, *J. Chromatogr.*, 125 (1976) 43.
9 A. Wehrli, U. Hermann and J. F. K. Huber, *J. Chromatogr.*, 125 (1976) 59.
10 H. Brusset, D. Depeyre and J. P. Pewtit, *Chromatographia*, 11 (1978) 287.
11 P. Gareil, L. Personnaz, J. P. Feraud and M. Caude, *J. Chromatogr.*, 192 (1980) 53.
12 A. W. J. de Jong, H. Poppe and J. C. Kraak, *J. Chromatogr.*, 209 (1981) 432.
13 B. Coq, G. Cretier and J. L. Rocca, *Anal. Chem.*, 54 (1982) 2271.
14 H. Poppe and J. C. Kraak, *J. Chromatogr.*, 255 (1983) 395.
15 P. Gareil, C. Durieux and R. Rosset, *Sep. Sci. Technol.*, 18 (1983) 441.
16 G. Cretier and J. L. Rocca, *Chromatographia*, 18 (1984) 623.
17 G. Cretier and J. L. Rocca, *Chromatographia*, 20 (1985) 461.
18 A. Jaulmes, C. Vidal-Madjar, H. Colin and G. Guiochon, presented at the *8th International Symposium on Column Liquid Chromatography, New York, May 20–25, 1984.*
19 J. Frenz and Cs. Horváth, *AIChE J.*, 31 (1985) 400.
20 M. Verzele and C. Dewaele, *LC Liq. Chromatogr. HPLC Mag.*, 3 (1985) 22.
21 J. E. Eble, P. E. Antle, R. L. Grob and L. R. Snyder, *J. Chromatogr.*, 384 (1986) 45.
22 B. L. Karger, L. R. Snyder and Cs. Horváth, *An Introduction to Separation Science*, Wiley-Interscience, New York, 2nd ed., 1979, pp. 110–116.
23 L. R. Snyder, *Principles of Adsorption Chromatography*, Marcel Dekker, New York, 1968, pp. 55–58.
24 A. Jaulmes, C. Vidal-Madjar, A. Ladurelli and G. Guiochon, *J. Phys. Chem.*, 88 (1984) 5378.
25 L. R. Snyder, in C. N. Reilley (Editor), *Advances in Analytical Chemistry and Instrumentation*, Vol. 3, Wiley-Interscience, New Yorki, 1964, p. 251 (see Fig. 14, p. 295).
26 S. Seshadri and S. N. Deming, *Anal. Chem.*, 56 (1984) 1567.
27 P. Gareil, L. Semerdjian, M. Caude and R. Rosset, *J. High Resolut. Chromatogr. Chromatogr. Commun.*, 7 (1984) 123.